International Journal of Theoretical Physics, Vol. 38, No. 10, 1999

Normalization in the Spinor Strong Interaction Theory and Strong Decay of Vector Meson $V \to PP$

F. C. Hoh[1]

Received May 28, 1999

The meson wave function in the spinor strong interaction theory is uniquely normalized on dimensional grounds, thus bypassing the fundamental problems in the normalization of Klein–Gordon (KG) and Bethe–Salpeter amplitudes for mesons. While the KG amplitude is proportional to $1/\sqrt{E}$, the present meson wave function is not and is thus flavor-independent. The confinement term is inactive for free mesons, but is activated when interacting with another hadron or charged lepton. The theory is applied to the strong decay of a two-quark vector meson into two pseudoscalar mesons $V \to PP$. The so-obtained and estimated decay rates are consistent with data, as are the ratios of these rates to the corresponding radiative decay $V \to P\gamma$ rates. These decay rates indicate a possible connection of the strong quark–quark coupling α_s with the electromagnetic coupling α via $\alpha_s = \alpha^{1/4} = 0.2923$. Contrary to the standard electroweak model (SM), the electromagnetic and weak couplings are detached from each other in connection with the absence of Higgs bosons, without altering the main results of the SM.

1. INTRODUCTION

The current mainstream theories of elementary particles are quantum chromodynamics (QCD) for strong interactions and the standard model (SM) for electroweak interactions [1]. These theories, about 25–30 years old, despite success in a large body of applications, have not been verified in some basic areas, e.g., the inability of QCD to demonstrate confinement and the absence of the Higgs boson in SM. They also incorporate a number of "fundamental parameters" whose values vary from case to case depending upon how they are fixed by data. Three basic examples are the QCD effective

Dragrunnsg. 9B, 75332 Uppsala, Sweden; email (at The Svedberg Laboratory, Uppsala University): hoh@tsl.uu.se.

0020-7748/99/1000-261 7$16.00/0

coupling α_s, the Cabbibo angle θ_c, and the Weinberg angle θ_w. Further, these theories suffer when considered from an aesthetic point of view.

It has not been possible to derive from the QCD Lagrangian, which contains quark fields, useful Lagrangians containing meson fields. Therefore, current predictions of low-energy hadronic data are based upon phenomenological Lagrangians [2, 3]. A vast literature exists on this subject. A large class of these are QCD-oriented, nonrenormalizable, chiral perturbation theories for application to light mesons [3, 4]. When the meson contains a very heavy quark, a new spin-flavor symmetry emerges from QCD and can be incorporated to apply to heavy mesons [5, 6].

Only local meson fields appear in these Lagrangians. Since mesons have finite size and internal structure, much physical content is irretrievably lost in such transitions to phenomenology. Undetermined parameters are introduced to compensate for such loss, to take into account various types of interaction couplings and to cancel divergences. As a result, there exists a large number of such phenomenological Lagrangians with many free parameters to be fixed by data. The applicability of some of these data is not self-evident and has not been fully demonstrated.

By the standard of quantum mechanics applied to atomic physics, the above difficulties clearly indicate that QCD and SM meet great difficulties in some basic aspects. That in spite of this they remain the mainstream theories is in part due to the lack of alternative theories that are as basic and as comprehensive.

A candidate that may become such an alternative was proposed a few years ago [7; hereafter denoted by I], developed [8], and applied to meson spectra [9]. The theory successfully accounts for confinement, the absence of ground-state scalar and axial vector mesons, the pseudoscalar meson masses, apart from those used as inputs, and approximately the vector meson masses. It further shows the nonexistence of the pseudoscalar isosinglets [U(1) problem] and the Higgs bosons.

When applied to the weak decay of flavored pseudoscalar mesons [10; hereafter denoted by II], the Cabbibo angle is correctly predicted. Further, the Weinberg angle was also predicted to be 30 deg in the limit of SU(3) flavor symmetry [11].

In this paper, physical assignments and interpretations of the formalism developed [7–10] as well as normalization of the meson wave functions are given. The theory is applied to the strong decay of a two-quark vector meson into two pseudoscalar mesons $V \rightarrow PP$. The sister process, the radiative decay $V \rightarrow P\gamma$, is analogously treated in an accompanying paper [12; hereafter denoted by III].

Based upon these results, it is conjectured that electromagnetic coupling α is related to the strong coupling α_s. Another independent conclusion is

that the electromagnetic coupling α is dissociated from the weak coupling characterized by the Fermi constant G. This, however, does not alter the successful results of purely leptonic interactions in SM. These points are considered in Section 9.

In Section 2, noninteracting, ground-state meson wave functions obey linear wave equations. The nonlinear confinement term is called into action when the meson is close to another hadron. A fundamental mesonic length is identified. Normalization of the meson wave function amplitudes is treated in Section 3, whereby the arbitrariness in the normalization constant in the current literature is removed and flavor independence of the meson wave functions is found.

Since $V \to PP$ involves four quarks, four-quark meson wave equations of approximative nature are constructed in Section 4 by extending the construction of the two-quark meson wave equations in the Appendix, reproduced from ref. 7. The four-quark meson wave equations have been converted into an action and the strong decay amplitude is derived in Section 5. In Section 6, a physical picture of the decay mechanism as well as the perturbed potential is given. The decay amplitude can be estimated explicitly if the decay products move nonrelativistically. Such decay rates are derived in Section 7 and applied to $V \to PP$ in Section 8, where the limits of their validity are given. The predictions are consistent with data and are compared to earlier work.

2. FREE AND CONFINED MESONS

The basic meson equations (A7)–(A9) are in spinor form. Dropping the internal function ξ, which characterizes flavor dependence, (A7) has been converted into vector form (I 6.4), reproduced in (III B1). For two-quark mesons without angular excitation and at rest, these equations have been reduced to radial equations (I 7.3), (I 7.4), (I 8.3), and (I 8.4), which have been collected into the form of (1), (3), and (4) of ref. 9:

$$\left(\frac{\partial^2}{\partial r^2} + \frac{2}{r}\frac{\partial}{\partial r} - \frac{J(J+1)}{r^2} + \Phi_{PJn} + \Lambda_{Jn}\right)\psi_{Jn}(r) = 0 \tag{2.1a}$$

$$\Phi_{PJn} = -\Phi'_{PJn} + d_m/r - \Phi_0 - e_m r^2 \tag{2.1b}$$

$$\Phi'_{PJn} = \frac{1}{6}\left[\int_0^r dr'\, r'^2 \psi_{Jn}^2(r')\left(3r + \frac{r'^2}{r}\right) + \int_r^\infty dr'\, r'\, \psi_{Jn}^2(r')(3r'^2 + r^2)\right] \tag{2.1c}$$

$$N_{cJn} = \int_0^\infty dr\, r^2 \psi_{Jn}^2(r) = 2[\Phi'_{PJn}/r]_{r\to\infty} \tag{2.1d}$$

$$4\Lambda_{Jn} = (E_{Jn} - Q^2 E_{emJ})^2 - (m_p + m_q)^2 \tag{2.1e}$$

Here, $J = 0, 1$ denotes pseudoscalar (0^-) and vector (1^-) mesons, respectively, n the radial quantum number, $\psi(r)$ is the meson wave function [see (III 3.1)] with $r \equiv |\mathbf{x}|$ denoting the interquark distance, m_p and m_q are the masses of quarks of flavors p and q, respectively, and d_m, Φ_0, and e_m are integration constants arising from (A9), as was mentioned below (I 7.1). E and Q are the energy and charge, respectively, of the meson. The electromagnetic mass $E_{\text{emo}} = 2.1$ Mev of the 0^- meson has been estimated from its electromagnetic radius [9, 13, 14].

For small 0^- meson momentum K_0 or $\varepsilon_0 = K_0/E_{00} << 1$ or (III B5), (2.1) still holds by virtue of (III B8a). Corrections to E_{00} are of order ε_0^2, as can be seen from (III B1). The same can be shown to hold for 1^- mesons.

Confinement is provided by Φ'_{PJn}, whose amplitude depends upon $|\psi_{Jn}|$ and thus is not fixed. This leads to the possibility of obtaining the same eigenvalue Λ_{Jn} for a continuous set of d_m and Φ_0 values and $|\psi_{Jn}|$ amplitudes or confinement strengths. Table 9 of ref. 9 gives for ground-state mesons four cases in this set, putting $e_m = 0$. For one of these cases, ψ_{J0} and Φ'_{PJ0} are plotted in Fig. 1 of ref. 9.

In addition to this arbitrariness, the nonlinear Φ'_{PJ0} in (2.1) prevents the application of the superposition principle to the Fourier components of the meson wave functions (III 3.1) in the laboratory space $\mathbf{X}$ (III A3a), so that one cannot build wave packets from them. These two aspects also hold for baryons, as is indicated in a comparison of (2.1) with (6.8), (6.9), (7.4), (7.5), and (5.1) of ref. 15.

The last aspect leads to a contradiction with observation; ground-state hadrons possess wave–particle duality properties, just like an electron does, and their wave functions have to obey the superposition principle, at least in a quasifree state of motion.

2.1. Free Mesons at Rest

Both difficulties of the last three paragraphs are removed by letting $|\psi_{J0}| \to 0$ when the meson moves freely and slowly and is far away from other hadrons. This corresponds to a minimization of the confinement potential energy $\Phi'_{PJ0} \to 0$; (2.1a) becomes a linear eigenvalue equation and the superposition principle can be applied to it. This linear equation together with the normalization (3.6) and (3.7) are solved to yield

$$\psi_{00} = A_0 \exp(-d_m r/2) \tag{2.2a}$$

$$\psi_{10} = A_1 r \exp(-d_m r/4) \tag{2.2b}$$

$$A_0 = \sqrt{d_m^3/8\pi\Omega} \tag{2.3a}$$

$$A_1 = \sqrt{d_m^5/3072\pi\Omega} \tag{2.3b}$$

$$\Lambda_{J0} = -[d_m/2(J+1)]^2 + \Phi_0 \tag{2.4}$$

where Ω can $\to\infty$ so that ψ_{J0} and $\Phi'_{PJ0} \to 0$ in that limit. No confinement term is needed for free mesons, just as a hydrogen atom by itself is stable. ψ_{00} corresponds to the ground-state hydrogen atom wave function and ψ_{10} to the radial part of the wave function of a hydrogen atom with unit angular momentum, but with no angular dependence associated with it.

2.2. Mesons Close to Other Hadrons: Confined Mesons

Under interaction, the hydrogen atom can disintegrate since there is no confining mechanism for its electron. This is no longer the case for hadrons; the confinement terms can be called into action to prevent their disintegration. The problem of a meson interacting with another hadron or charged lepton has not been treated in the framework of the spinor strong interaction theory. Therefore, only a qualitative account of such confinement is given below.

When another hadron approaches the meson, the quarks in the meson start to experience the massless pseudoscalar or scalar forces from the quarks in the approaching hadron, according to equations of the type of (A1) and (A3a) and of (2.1) and (2.4a) in [15]. These forces produce a perturbation in ψ_{J0}, which originally ≈ 0 and is uniformly distributed in the laboratory space $\mathbf{X}$ for large Ω in (2.3). This perturbation causes that the resulting ψ_{J0} now has a gradient in $\mathbf{X}$ in the interaction region and therefore is no longer zero, but is finite there. This in turn renders the confining potential Φ'_{PJ0} in (2.1c) finite and confinement becomes active in (2.1a).

This tendency is reinforced as the hadron moves closer to the meson. But then the confining potential Φ'_{PJ0} is no longer of the simple form of (2.1c), but will depend upon $\mathbf{X}$, since the meson wave function products on the right of (A9) now depend upon $\mathbf{X}$. Another way to see it is that the meson wave function ψ_{J0}, originally spread out in a large volume $\Omega \to \infty$, is pushed back by the approaching hadron so that Ω is reduced to some finite volume in the interaction region according to the reverse of (3.7b). Thus, (2.3), hence (2.2) and Φ'_{PJ0}, become finite and confinement takes place.

2.3. Excited Mesons

The confinement term Φ'_{PJ0} has already been in effect for radially excited mesons represented by $n > 0$ in (2.1), as demonstrated in Figs. 2 and 3 of ref. 9. The zero confinement formulas (2.4) and (2.1e) together with the quark masses of Table 1 of ref. 9 ($m_u = 0.6592$ GeV, . . .) cannot predict the masses of the radially excited $\pi(1300)$ and other such mesons in Tables 5 and 7 of ref. 9. For these states, therefore, the superposition principle no

longer holds and one cannot build wave packets for these excited states. This may not contradict data, however, since these states have very large widths and cannot be observed as freely moving particles. The same reasoning also applies to the orbitally excited mesons of Tables 6 and 8 of ref. 9 because these high-mass states also have large widths.

2.4. Fundamental Mesonic Length

It is well known that the differences of the squares of the masses of the vector and pseudoscalar mesons are nearly the same, independent of their quark content [16]. This fact has been used to determine the integration constant d_m in Section 10 of I from (2.4). Insertion of six pseudoscalar meson masses into (2.1e) and (2.4) has led to a determination of the five quark masses and the other integration constant Φ_0 as well as successful predictions the remaining mesons consisting of two quarks [9] (η and η' consist of six quarks). For free mesons, (I 10.2) and the second line in Table 9 of ref. 9 give

$$d_m = 0.864 \text{ GeV}, \qquad d_m^{-1} = 1.435 \text{ fm} \tag{2.5a}$$

$$\Phi_0 = -0.24455 \text{ GeV}^2 \tag{2.5b}$$

which are independent of flavor.

In a free meson, the quarks are confined by the d_m/r term in (2.1b), just as the electron is confined by the Coulomb potential e^2/r in a hydrogen atom. This comparison suggests that $1/d_m$ may be identified as the fundamental mesonic length constant or d_m as the fundamental mesonic energy scale, just as e is the fundamental charge constant in electromagnetic interactions. It provides a reference length scale for mesonic phenomena, analogous to the way e, together with the electron mass, controls the hydrogen atom radius, which provides a reference length scale for atomic phenomena.

This is so because the original strong coupling constant g_q^2 of (A3) has been elevated into the source term on the right side of (A9) for the confining potential via (A5). Its place is taken by d_m/r, which is proportional to the Green's function of a second-order equation like (A3a), but is also an integration constant type of term in a solution (2.1b), (2.1c) to the fourth-order potential equation (A9).

There is also a confining integration constant type of term $e_m r^2$ in (2.1b) which is a harmonic type of potential, contrary to the linear type of potential supported by data. It has therefore been put to zero. Likewise, the integration constants $d_{11} = d_{13}$, $d_{10} = d_{30}$, and $d_1 = d_3$ in the intrabaryonic potentials (6.8) and (7.5) of ref. 15 may lead to fundamental baryonic constants.

2.5. Meson Radii

As is seen from (2.2), the meson radii are determined by d_m. With (2.5a) and (2.2), the strong interaction radii of free pseudoscalar and vector mesons are

$$r_0 = \ln 2/d_m \approx 1 \text{ fm}, \qquad \langle r_0 \rangle = 1/d_m \tag{2.6a}$$

$$\langle r_1 \rangle = 4/d_m \approx 5.7 \text{ fm} \tag{2.6b}$$

where r_0 is the half-width of ψ_{00}^2 and $\langle r_1 \rangle$ refers to the maximum of ψ_{10}. It is known that the strong interaction radius of a pseudoscalar meson is of the same magnitude as its electromagnetic radius (see also Section 9.1), which has been measured to be 0.6–0.7 fm for K and π [13, 14]. These values are of the same order as r_0 in (2.6a) and provide a qualitatitive support for the present theory.

The large vector meson radius (2.6b), corresponding to that of the first excited state of a hydrogen atom, is a unique feature of the spinor strong interaction theory. A direct measurement of this radius will provide a crucial test of the present theory.

The confinement term Φ'_{PJ0} will obviously reduce the meson radii. A numerical integration of (2.1a)–(2.1c) has been performed and the confinement potential and wave functions are displayed in Figs. 1 and 2 of I. The meson radii reported below these figures are smaller than those of (2.6), as expected. The same kind of numerical integration has also been been carried out for radially excited states with $n = 1$ and 2 and some confinment strength. Figures 2 and 3 of ref. 9 show that the meson radii become fairly large, of the magnitude of 15–30 fm.

3. NORMALIZATION OF MESON WAVE FUNCTIONS

The amplitudes (2.3) are determined by a further development of the normalization procedure of the Appendix of ref. 8 and Section 7 of II. Following the last reference, the conventional normalization procedure for a Klein–Gordon (KG) wave function ψ_{KG} is used as a model.

3.1. Klein–Gordon Wave Function Amplitude

Multiply the KG equation for a free particle by ψ^*_{KG} and subtract it from its complex conjugate. After a rearrangement, one finds

$$\psi_{\text{KG}} = A_{\text{KG}} \exp(-\mathrm{i}EX^0 + i\bar{\bar{K}}\bar{\bar{X}}) \tag{3.1a}$$

$$\frac{\partial}{\partial X^\mu}\left(\psi_{\text{KG}} \frac{\partial}{\partial X^\mu} \psi^*_{\text{KG}} - \text{c.c.}\right) = 0 \tag{3.1b}$$

Integration of (3.1b) over $\mathbf{X}$ leads to

$$\frac{\partial}{\partial X^0} N_{\mathrm{KG}} = 0, \qquad N_{\mathrm{KG}} = \Omega A_{\mathrm{KG}}^2 2iE, \qquad \Omega = \int d^3 \bar{\bar{X}} \tag{3.2}$$

If the first of (3.2) is further integrated over X^0, it will have the same dimension as the action of this KG particle and will be a dimensionless Lorentz scalar. Therefore, N_{KG} is also a Lorentz scalar and, for instance, cannot depend linearly upon E, which is the time component of a four-vector. Since there is no natural physical constraint on N_{KG}, it is conventionally chosen as

$$N_{\mathrm{KG}} = i \tag{3.3}$$

so that (3.2) yields

$$A_{\mathrm{KG}} = 1/\sqrt{2E\Omega} \tag{3.4}$$

which is the form used throughout the literature. Since $E < 0$ is possible, there is no positive norm; N_{KG} can be any number. This arbitrariness led to some debate during the early development of quantum mechanics. This remains an unsettled but ignored issue to the present time.

3.2. Meson Wave Function Amplitude and Flavor Independence

Following the procedure leading to (3.1b), drop the ξ's in (A7a) and multiply it by $\chi_{\dot{a}}^{\dot{e}} = (\chi_a^e)^*$. Subtract the resulting equation from the complex conjugate of (A8) multiplied by $\psi_{\dot{a}}^{\dot{c}}$, dropping the ξ's there. This was carried out earlier and led to (A2) of ref. 8 or (II 7.2):

$$\partial_{\mathrm{I}}^{\dot{b}a} \chi_{\dot{a}}^{\dot{e}} \partial_{\mathrm{II}\dot{e}f} \chi_{\dot{b}}^{f} - \partial_{II}^{\dot{a}d} \psi_{\dot{d}}^{\dot{c}} \partial_{\mathrm{I}\dot{b}c} \psi_{\dot{a}}^{\dot{b}} = (\partial_{\mathrm{I}}^{\dot{b}a} \chi_{\dot{a}}^{\dot{e}})(\partial_{\mathrm{II}\dot{e}f} \chi_{\dot{b}}^{f}) - (\partial_{\mathrm{II}}^{\dot{a}d} \psi_{\dot{d}}^{\dot{c}})(\partial_{\mathrm{I}\dot{b}c} \psi_{\dot{a}}^{\dot{b}}) \tag{3.5}$$

Both terms on the right side cancel out for mesons at rest generally, as was pointed out in (A2) and (A3) of ref. 8. Here, this can be shown by substituting (III 3.1) with K_J, $\omega_{J\mathbf{K}} = 0$, (III 3.2) with $a_{J\mathbf{K}} = 1$ and $a_{J\mathbf{K}}^{(1)} = 0$, (III 3.6), (III A3), (2.1), and (2.2) into the right of (3.5). Substituting the same set into the left side of (3.5) and integrating it over $\mathbf{x}$ and $\mathbf{X}$ leads to

$$\frac{\partial}{\partial X^0} N_{mJ} = 0, \qquad N_{mj} = -iE_{J0}\, \Omega \int d^3 \bar{\bar{x}} \psi_{J0}^2(r), \qquad \Omega = \int d^3 \bar{\bar{X}} \tag{3.6}$$

which is (A3) of ref. 8 and the analog of (3.2).

If the fisrt of (3.6) is integrated over X^0 and x^0, it takes the dimension of the action (III A4) or (5.1) below and becomes a dimensionless Lorentz scalar. Therefore, N_{mJ} must have dimension energy and be the time component of a four-vector and hence differs basically from N_{KG}. Since the only energy constant associated with the meson is its energy E_{J0}, N_{mJ} must be E_{J0} times a constant Lorentz scalar and can be put in the form

$$N_{mJ} = -iE_{J0}\Omega/\Omega_c \tag{3.7a}$$

where Ω_c is interpreted as the volume in the laboratory space **X** occupied by the meson wave functions which are confined by the finite amplitudes in (2.1a), (2.1c), and (2.1d). In the limit of free mesons, these amplitudes vanish as

$$\Omega_c \to \Omega \to \infty \tag{3.7b}$$

The appearance of i in (3.7a) identifies it with the time component of a four-vector.

The normalization (3.7a) is the consequence of the appearance of the relative time x^0 in a Lorentz-invariant formulation. It answers at the same time, at least in part, the two seemingly unrelated questions raised by Wick [17] on the Bethe–Salpeter equation, namely the lack of a positive-definite norm and the significance of the relative time. As is shown in (3.10) below, the gauge boson mass M_w is also fixed by a relative time scale.

The choice of i in (3.3) is not aesthetically appealing. This and the arbitrariness of N_{KG} are avoided by the specific fixation of (3.7a). This in turn implies that the application of the Klein–Gordon equation with the choice (3.3) in the literature lacks firm theoretical foundation and can lead to erroneous conclusions. Two cases are mentioned here. Combining (3.6), (3.7), and (2.2) leads to (2.3), which does not depend upon E_{J0}, contrary to A_{KG} in (3.4). This important difference makes possible the prediction of the Cabbibo angle (II 11.4), which, at least in the meson sector, is not a fundamental parameter to be fixed by other data, as is the case in the standard electroweak model.

Further, (3.4) shows that all mesons will have different amplitudes dependent upon their different energies and flavors. In contrast, (2.3) does not depend upon energy, so that the meson wave function is flavor independent. This independence converts (2.1d) to

$$N_{c10} = N_{c00} \tag{3.8}$$

which has been employed to obtain Table 9 of ref. 9. This flavor independence is consistent with that of d_m in (2.5a). Both are required for the flavor independence of (2.1a).

3.3. Nonrelativistic Mesons

The results of Section 3.2 were derived for mesons at rest for which the coupled second-order equations (III B1) are decoupled and reduce to (2.1a). For mesons in motion, $\mathbf{K}_J \neq 0$ in (III 3.1) and the singlet and triplet parts in (III B1) couple, rendering an analytic solution complicated. The

situation is entirely analogous to that of the coupling of the small to large Dirac wave function components by motion; the singlet (triplet) parts in (III B1) represent large (small) components for pseudoscalar mesons and vice versa for vector mesons.

It will be estimated below that the normalization conditions (3.6)–(3.8) also hold to order $\varepsilon_0 = K_0/E_{00}$ (III B5), i.e., for nonrelativistic pseudoscalar mesons. That (2.1) holds to this approximation has been pointed out below it. The small triplet wave functions in (III B1) are determined by (III B8) to order ε_0. These equations are also not simply solved, but have been treated by a dimensional analysis in the heavy meson limit $E_{00} >> d_m$ of (III B11). The results are given by (III B14), and are also self-consistent to order ε_0^2, as is indicated by (III B17).

Equations (III B14) and (III B16) are inserted into (3.5). The calculation is straightforward and will not be reproduced here. It shows that the right side of (3.5) vanishes to order ε_0. The left side receives a contribution via $E_{00} \to E_{00} + (d_m/E_{00})\, \hat{r}\mathbf{K}_0$ for the limit (III B11a), dropping the ε_0^2 terms. Here, $\hat{r} = \mathbf{x}/|\mathbf{x}|$. Putting $d_m/E_{00} \approx \varepsilon_0$ for this limit, this contribution is also of order ε_0^2 and can be dropped. Thus, (3.6)–(3.8) for $J = 0$ and (2.3a) hold to order ε_0 for heavy mesons (III B11) from a dimensional analysis point of view. A similar conclusion can be obtained by an analogous treatment for the opposite of (B11), i.e., for light mesons. Therefore, it is estimated that (3.6)–(3.8) also hold for meson masses between these limits, i.e., for nonrelativistic pseudoscalar mesons of arbitrary mass.

3.4. Normalization in Weak Decay Processes

Under Sections 3.2 and 3.3 the integrals over the relative time x^0 cancel out in the actions (III 2.1) and (5.1) below. This is no longer the case in weak decays, in which x^0 can appear in the initial meson state, but not in the final lepton state. This together with a more transparent handling of such an integral over $\mathbf{X}$ lead to an ansatz of the type (II 3.1)–(II 3.3),

$$\psi^{a\dot{b}} \to \psi^{a\dot{b}} \exp(-(x^0/\tau_0)^2 - \bar{X}^2/L_M^2) \tag{3.9a}$$

$$\Omega = \int d^3\bar{X} \to \int d^3\bar{X} \exp(-2\bar{X}^2/L_M^2) = (\pi/2)^{3/2} L_M^2 \tag{3.9b}$$

$$\int dx^0 \to \int dx^0 \exp(-2(x^0/\tau_J)^2) = (\pi/2)^{1/2} \tau_J \tag{3.9c}$$

where τ_0 is a large relative time scale of the quarks and L_M a large cutoff length. With (3.9), the action (5.1) below is neither Lorentz nor gauge invariant; valid results are obtained only for large values of these parameters. This ansatz leads to the gauge boson mass (II 5.2b),

$$M_W^2 = \frac{\pi\sqrt{\pi}}{4} g^2 N_{c00}\tau_0 = (80.33\ \text{GeV})^2 \tag{3.10}$$

where g is the weak charge in (II 2.3d) and the relative energy $\omega_0 \to 0$ in (II 2.9) and (II 3.2), as is suggested below (5.2). A factor of $1/\sqrt{8}$ has been introduced into (3.10), according to (9.2) of ref. 11. However, no such integral over x^0 is present in the normalization condition (II 7.3), the equivalent of (3.6) and (II 7.4),

$$N_e = 4\pi N_{c00} E_{00} \Omega \tag{3.11}$$

which is equivalent to N_{m0} of (3.7) and hence is equal to iE_{00}. Application of this result to (II 6.5) would lead to a decay rate in disagreement with data.

These difficulties, not realized as such in Section 7 of II, are removed by introducing the τ_0 factor in (3.9a) and (3.9c) into (II 2.8) and integrating the so-modified (II 7.3) over x^0. Equations (II 7.4) and (3.11) are now altered to

$$N_d = 4\pi\ \sqrt{\pi/2} N_{c00}\tau_0 E_{00}\Omega = 4M_W^2 E_{00}\Omega/g^2 \tag{3.12}$$

where (3.10) has been consulted.

Now N_d is a large, dimensionless Lorentz scalar and thus cannot depend linearly upon a time component of a four-vector like E_{00}. The decay volume Ω in (3.11) and (3.12) is a representation of a δ-function, like that in (7.3b) below. Combining (3.12), (3.10), and (II 6.4) leads to the decay rate

$$\Gamma(K^+, \pi^+ \to \mu^+\nu) = 8\sqrt{2}\,\frac{N_d G^3 m_\mu^2}{\pi^4 L_M^6 E_{00}}\left(1 - \left(\frac{m_\mu}{E_{00}}\right)^2\right)^2 \tag{3.13}$$

which replaces (II 6.5) and (II 10.4). The prediction of the ratio of the K and π weak decay rates in II, without introducing any Cabbibo angle, remains unchanged by (3.13), which is finite if

$$N_d = M_M^6 L_M^6 \tag{3.14}$$

where M_{dW} is some mass scale of the order of 1.4 Gev. As was pointed out below (II 11.5), the pion decay constant $F \cos\theta_c$ there is essentially the ratio between two large constants N_d and L_M^6.

Similarly, the relative time scale $\tau_0 \propto M_W^2\Omega$ according to (3.10), (2.1d), (2.2a), and (2.3a). Conversely, M_W^2 is basically the ratio of two large quantities, τ_0 and Ω. Also, N_f of (II B6) is, like N_d, a large Lorentz scalar $\propto L_M^6$. For free mesons, however, the amplitude A_d in (II B6) is of the type (2.3), so that $N_f \propto L_M^3$.

4. CONSTRUCTION OF QUSAI-FOUR-QUARK MESON EQUATIONS

In the simplest OZI rule obeying decay of a vector meson into two pseudoscalar mesons, four quarks are involved; quark A of flavor p and antiquark B of flavor $\bar{r}$ forming the two-quark vector meson and a pair comprising quark C of flavor q and antiquark D of flavor $\bar{q}$ created from the vacuum and considered as perturbation initially. The vector meson AB decays into the two pseudoscalar mesons AD and CB or AB and CD.

The method of construction of the two-quark vector meson given in the Appendix is extended to apply to the four-quark case under the following restricted conditions. The wave functions for the quark C and antiquark D are the same as those in (A1) and (A2), except for the labels and I $\rightarrow$ III and II $\rightarrow$ IV for the designation of new coordinates for C and D. Consider the case that the C and D amplitudes are small relative to those for the quarks A and B and that the quarks A (B) and C (D) are close to each other so that $x_{III} \approx x_I$, $z_{III} \approx z_I$, $x_{IV} \approx x_{II}$, and $z_{IV} \approx z_{II}$. In this region, one may consider that the wave function for quark A is augmented by a perturbed wave function of quark C according to

$$\chi_{Ab}(x_I)\xi^p_A(z_I) + \chi_{Cb}(x_I)\xi^q_C(z_I), \qquad \psi^b_A(x_I)\xi^p_A(z_I) + \psi^b_C(x_I)\xi^q_C(z_I) \tag{4.1}$$

A similar set holds for the antiquarks B and D. Instead of two separate quarks, they are considered as a mixed state so that the genuine four-quark problem is reduced to a tractable two-quark one.

Equations (A1)–(A3) generalized to the four-quark case now read

$$\partial_I^{ab}(\chi_{Ab}(x_I)\xi^p_A(z_I) + \chi_{Cb}(x_I)\xi^q_C(z_I)) = i(m_{Aop}(z_I, \partial/\partial z_I) - V_{BD}(x_I))(\psi^b_A(x_I)\xi^p_A(z_I) + \psi^b_C(x_I)\xi^q_C(z_I)) \tag{4.2a}$$

$$\partial_{I\dot{c}b}(\psi^b_A(x_I)\xi^p_A(z_I) + \psi^b_C(x_I)\xi^q_C(z_I)) = i(m_{Aop}(z_I, \partial/\partial z_I) + V_{BD}(x_I))(\chi_{A\dot{c}}(x_I)\xi^p_A(z_I) + \chi_{C\dot{c}}(x_I)\xi^q_C(z_I)) \tag{4.2b}$$

$$\partial_{II\dot{e}f}(\chi^f_B(x_{II})\xi_{Br}(z_{II}) + \chi^f_D(x_{II})\xi_{Dq}(z_{II})) = i(m_{Bop}(z_{II}, \partial/\partial z_{II}) - V_{AC}(x_{II}))(\psi_{B\dot{e}}(x_{II})\xi_{Br}(z_{II}) + \psi_{D\dot{e}}(x_{II})\xi_{Dq}(z_{II})) \tag{4.3a}$$

$$\partial^{\dot{d}\dot{e}}_{II}(\psi_{B\dot{e}}(x_{II})\xi_{Br}(z_{II}) + \psi_{D\dot{e}}(x_{II})\xi_{Dq}(z_{II})) = i(m_{Bop}(z_{II}, \partial/\partial z_{II}) + V_{AC}(x_{II}))(\chi^d_B(x_{II})\xi_{Br}(z_{II}) + \chi^d_D(x_{II})\xi_{Dq}(z_{II})) \tag{4.3b}$$

$$\Box_I V_{BD}(x_I) = \frac{i}{4} g_q^2[(\psi^b_B(x_I) + \psi^b_D(x_I))(\chi_{Bb}(x_I) + \chi_{Db}(x_I)) - \text{c.c.}] \tag{4.4a}$$

$$\Box_{II} V_{AC}(x_{II}) = \frac{i}{4} g_q^2[(\psi^a_A(x_{II}) + \psi^a_C(x_{II}))(\chi_{Aa}(x_{II}) + \chi_{Ca}(x_{II})) - \text{c.c.}] \tag{4.4b}$$

We follow the procedure in the Appendix and multiply together (4.2a) and (4.3a). This leads to a equation similar to (A4), but with four product wave functions on each side instead of one as in (A4). Each of the resulting products is generalized to a nonseparable meson wave function, distinguished from each other by the subscripts AB, AD, CB, and CD, or to internal operators in the same way as in (A5) and (A6). Since only three mesons are involved in $V \to PP$, one of the four product meson wave functions is dropped. This can be represented by dropping CD, the created $\bar{q}q$ pair, so that (i) $AB \to AD + CB$; $D^{*+} \to D^0\pi^+$ is an example. Alternatively, (ii) $AB \to AB + CD$; $D^{*+} \to D^+\pi^0$ provides an example. In the following, only (i) will be considered. The interchange $D \leftrightarrow B$ among the decay products turns this case to (ii), which will be applied. The resulting meson equation corresponding to (A7a) reads

$$\partial_{\mathrm{I}}^{ab}\partial_{\mathrm{II}\dot{e}f}(\chi^f_{ABb}(x_{\mathrm{I}}, x_{\mathrm{II}})\xi^p_r(z_{\mathrm{I}}, z_{\mathrm{II}}) + \chi^f_{ADb}(x_{\mathrm{I}}, x_{\mathrm{II}})\xi^p_q(z_{\mathrm{I}}, z_{\mathrm{II}}) + \chi^f_{CBb}(x_{\mathrm{I}}, x_{\mathrm{II}})\xi^q_r(z_{\mathrm{I}}, z_{\mathrm{II}}))$$

$$= (\Phi_{P4}(x_{\mathrm{I}}, x_{\mathrm{II}}) - m_{2op}) \begin{bmatrix} \psi^a_{ABe}(x_{\mathrm{I}}, x_{\mathrm{II}})\xi^p_r(z_{\mathrm{I}}, z_{\mathrm{II}}) + \\ \psi^a_{ADe}(x_{\mathrm{I}}, x_{\mathrm{II}})\xi^p_q(z_{\mathrm{I}}, z_{\mathrm{II}}) + \psi^a_{CBe}(x_{\mathrm{I}}, x_{\mathrm{II}})\xi^q_r(z_{\mathrm{I}}, z_{\mathrm{II}}) \end{bmatrix} \tag{4.5a}$$

where Φ_{P4} is defined in (4.6a) below. Multiplying together (4.2b) and (4.3b) and following the same procedure gives

$$\partial_{\mathrm{I}cb}\partial^{d\dot{e}}_{\mathrm{II}}(\psi^b_{AB\dot{e}}(x_{\mathrm{I}}, x_{\mathrm{II}})\xi^p_r(z_{\mathrm{I}}, z_{\mathrm{II}}) + \psi^b_{AD\dot{e}}(x_{\mathrm{I}}, x_{\mathrm{II}})\xi^p_q(z_{\mathrm{I}}, z_{\mathrm{II}}) + \psi^b_{CB\dot{e}}(x_{\mathrm{I}}, x_{\mathrm{II}})\xi^q_r(z_{\mathrm{I}}, z_{\mathrm{II}}))$$

$$= (\Phi_{P4}(x_{\mathrm{I}}, x_{\mathrm{II}}) - m_{2op}) \begin{bmatrix} \chi^d_{AB\dot{c}}(x_{\mathrm{I}}, x_{\mathrm{II}})\xi^p_r(z_{\mathrm{I}}, z_{\mathrm{II}}) + \\ \chi^d_{AD\dot{c}}(x_{\mathrm{I}}, x_{\mathrm{II}})\xi^p_q(z_{\mathrm{I}}, z_{\mathrm{II}}) + \chi^d_{CB\dot{c}}(x_{\mathrm{I}}, x_{\mathrm{II}})\xi^q_r(z_{\mathrm{I}}, z_{\mathrm{II}}) \end{bmatrix} \tag{4.5b}$$

Multiplying together (4.4a) and (4.4b) and following the same procedure leading to (A9) leads to

$$-V_{BD}(x_{\mathrm{I}})V_{AC}(x_{\mathrm{II}}) \to \Phi_{P4} = \Phi_{PAB} + \Phi_{1P4} \tag{4.6a}$$

$$\Box_{\mathrm{I}}\Box_{\mathrm{II}}\Phi_{PAB}(x_{\mathrm{I}}, x_{\mathrm{II}}) = \tfrac{1}{8}\mathrm{Re}(\psi^a_{ABb}(x_{\mathrm{II}}, x_{\mathrm{I}})\chi^b_{ABa}(x_{\mathrm{II}}, x_{\mathrm{I}})) \tag{4.6b}$$

$$\Box_{\mathrm{I}}\Box_{\mathrm{II}}\Phi_{1P4}(x_{\mathrm{I}}, x_{\mathrm{II}}) \tag{4.6c}$$

$$= \frac{1}{16}\begin{bmatrix} \psi^a_{ADb}(x_{\mathrm{II}}, x_{\mathrm{I}})\chi^b_{CBa}(x_{\mathrm{II}}, x_{\mathrm{I}}) + \psi^a_{CBb}(x_{\mathrm{II}}, x_{\mathrm{I}})\chi^b_{ADa}(x_{\mathrm{II}}, x_{\mathrm{I}}) + \\ \psi^a_{CBb}(x_{\mathrm{II}}, x_{\mathrm{I}})\chi^b_{CBa}(x_{\mathrm{II}}, x_{\mathrm{I}}) + \psi^a_{ADb}(x_{\mathrm{II}}, x_{\mathrm{I}})\chi^b_{ADa}(x_{\mathrm{II}}, x_{\mathrm{I}}) + \\ \psi^a_{ABb}(x_{\mathrm{II}}, x_{\mathrm{I}})\chi^b_{CBa}(x_{\mathrm{II}}, x_{\mathrm{I}}) + \psi^a_{CBb}(x_{\mathrm{II}}, x_{\mathrm{I}})\chi^b_{ABa}(x_{\mathrm{II}}, x_{\mathrm{I}}) + \\ \psi^a_{ABb}(x_{\mathrm{II}}, x_{\mathrm{I}})\chi^b_{ADa}(x_{\mathrm{II}}, x_{\mathrm{I}}) + \psi^a_{ADb}(x_{\mathrm{II}}, x_{\mathrm{I}})\chi^b_{ABa}(x_{\mathrm{II}}, x_{\mathrm{I}}) \end{bmatrix} + \text{c.c.}$$

Multiplying (4.5a) and (4.5b) by $\xi^r_p(z_{\mathrm{I}}, z_{\mathrm{II}})$, $\xi^q_p(z_{\mathrm{I}}, z_{\mathrm{II}})$, and $\xi^r_q(z_{\mathrm{I}}, z_{\mathrm{II}})$ and making use of (III A5) and (III A9) leads to

$$\partial_{\mathrm{I}}^{ab}\partial_{\mathrm{II}\dot{e}f}\chi^{f}_{AB\dot{b}}(x_{\mathrm{I}}, x_{\mathrm{II}}) = (\Phi_{P4}(x_{\mathrm{I}}, x_{\mathrm{II}}) - M^2_{AB})\psi^{a}_{AB\dot{e}}(x_{\mathrm{I}}, x_{\mathrm{II}}) \tag{4.7a}$$

$$\partial_{\mathrm{I}\dot{c}b}\partial_{\mathrm{II}}^{d\dot{e}}\psi^{b}_{AB\dot{e}}(x_{\mathrm{I}}, x_{\mathrm{II}}) = (\Phi_{P4}(x_{\mathrm{I}}, x_{\mathrm{II}}) - M^2_{AB})\chi^{d}_{AB\dot{c}}(x_{\mathrm{I}}, x_{\mathrm{II}}) \tag{4.7b}$$

$$(4.7) \text{ with } AB \to AD \tag{4.8}$$

$$(4.7) \text{ with } AB \to CB \tag{4.9}$$

where (A7b) and (A7c) have been employed with $M_{AB} = M_m$. All other product equations vanish in the same manner as the corresponding ones do in the Appendix.

Equations (4.6)–(4.9) form a set of seven equations for the seven variables ψ_{AB}, χ_{AB}, $AB \to AD$, $AB \to CB$, and Φ_{P4}. The various meson wave functions for AB, AD, and CB are coupled strongly in Φ_{P4} of (4.6), and contain new and strong interactions not present in the two-quark meson equations (A7)–(A9).

Equations (4.6b) and (4.7a) are of zeroth order and account for the vector meson AB. Equations (4.8)–(4.9) and the first two terms on the right of (4.6c) are of higher order. They describe the decay products AD and CB.

5. ACTION FOR V $\to$ PP DECAY AND DECAY AMPLITUDE

Equation (4.7) is converted into the form of an action (III A4) or (5.1) of ref. 8 with some of the symbols changed;

$$S_M = \int d^4x_{\mathrm{I}}\, d^4x_{\mathrm{II}}\, \frac{1}{4}\left\{\begin{array}{c}(\partial_{\mathrm{I}}^{\dot{b}a}\chi^{\dot{e}}_{ABa})(\partial_{\mathrm{II}\dot{e}f}\chi^{f}_{AB\dot{b}}) + (\partial_{\mathrm{II}}^{\dot{b}a}\psi^{\dot{e}}_{ABa})(\partial_{\mathrm{I}\dot{e}f}\psi^{f}_{AB\dot{b}}) + \text{c.c} \\ + 2(\Phi_{P4} - M^2_{AB})(\psi^{\dot{c}}_{ABd}\chi^{d}_{AB\dot{c}} + \text{c.c.})\end{array}\right\} \tag{5.1}$$

This action is entirely similar to the actions (III 2.1) for the radiative decay $\mathrm{V} \to \mathrm{P}\gamma$ and (II 2.4) for the weak decay $\mathrm{K} \to \mu\nu$ and will be treated in an analogous manner. Laboratory coordinate X and relative coordinate x are introduced in (III A3a).

The vector meson wave function is written as a special case of (III 3.1),

$$\psi^{ab}_{AB}(x_{\mathrm{I}}, x_{\mathrm{II}}) = (a^{(0)}_{AB} + a^{(1)}_{AB}(X^0))[\exp(-iE_{10}X^0)](-\bar{\sigma}^{ab}\bar{\psi}_{10}(\bar{x})) \tag{5.2a}$$

$$(5.2a) \text{ with } \psi \to \chi \tag{5.2b}$$

The relative energy $\omega_{\mathbf{JK}} = 0$ has been set in (5.2) for similar reasons as those given above (III 4.2). The annihilation operator and initial and final states are defined, as in (II 4.3), by

$$a^{(0)}_{AB}\exp(-iE_{10}X^0) \to a_{AB}, \qquad |i\rangle = |V_{AB}\rangle$$
$$a_{AB}|V_{AB}\rangle = |0\rangle, \qquad \langle f| = \langle 0| \tag{5.3}$$

$a^{(1)}_{AB}(X^0)$ is a first-order quantity varying slowly with the time X^0 and characterizes the decay of V_{AB}, the vector meson AB.

Equation (5.1) is thus divided into a zeroth-order part, accounting for V_{AB} at rest, and a perturbational part consisting of terms of type (i) and type (ii), as in III Section 2. The type (i) terms are linear in $a^{(1)}_{AB}(X^0)$ and type (ii) terms are linear in the perturbed potential Φ_{1P4} of (4.6c).

The treatment of type (i) terms proceeds in the same way as in III Section 3 and II Section 4 with the modifications indicated in (5.2) and (5.3). Sandwiching these terms between $\langle f|$ and $|i\rangle$ leads to the equivalent of (III 3.5) or (II 4.4),

$$-i\frac{1}{2}E_{10}S_{fi}\Omega_N\int d^4x\,|\bar{\psi}_{10}(\bar{x})|^2, \qquad \Omega_N=\int d^3\bar{X} \tag{5.4a}$$

$$S_{fi}=\langle 0|a^{(1)}_{AB}(\infty)(\exp(iE_{10}\infty))a_{AB}|V_{AB}\rangle = a^{(1)}_{AB}(\infty)(\exp(iE_{10}\infty)) \tag{5.4b}$$

Sandwiching the type (ii) terms in (5.1) between $\langle f|$ and $|i\rangle$ and making use of (5.2) and (5.3) and (III A3a) leads to

$$2\int d^4X\,d^4x\,\Phi_{1P4}(\exp(iE_{10}X^0))|\bar{\psi}_{10}(\bar{x})|^2 \tag{5.5}$$

Equating (5.4a) to the negative of (5.5) yields the decay amplitude

$$S_{fi}=$$

$$-i\frac{4}{E_{10}\Omega_N}\int d^4X\,d^3\bar{x}\;\Phi_{1P4}(\exp(iE_{10}X^0))|\bar{\psi}_{10}(\bar{x})|^2\Big/\int d^3\bar{x}\;|\bar{\psi}_{10}(\bar{x})|^2 \tag{5.6}$$

6. PHYSICAL PICTURE AND PERTURBED POTENTIAL

The solution to the zeroth-order potential Φ_{PAB} of (4.6b) has been given by (2.1b) with J, $n=1$, 0 and Φ'_{PJ0}, $e_m=0$, according to Section 2.1 and the discussion above it. A perturbational treatment holds if in (4.6)

$$|\Phi_{1P4}| \ll |\Phi_{PAB}| \approx |d_m/\langle r_1\rangle - \Phi_0| \cong (0.19+0.24)\ \text{GeV} \tag{6.1}$$

which will be justified below.

Only the first two source terms + c.c. on the right of (4.6c) will contribute to Φ_{1P4}. These terms are associated with the decay products AD and CB having a total energy E_{10} in (5.6); the remaining terms will drop out upon integration over X^0 because they are associated with total energies differing from E_{10}.

6.1. Physical Picture

In the rest frame of the vector meson AB, $\psi_1(r) = |\bar{\psi}_{10}(r)|$ in (III 3.6) and (5.2a) is given by (2.2b) and (2.3b) and is evenly distributed in a large volume Ω with vanishing amplitude A_1. A virtual quark–antiquark pair CD is initially created in AB. To be specific, let $BA \to \bar{u}c$ and $DC \to dd$ and choose alternative (ii) above (4.5a) to represent $D^{*0} \to D^0\pi^0$. This initial stage is illustrated in Fig. 1a. The c and d quarks are about 6 fm apart according to (2.6b), much greater than the d–d distance. Therefore, (4.1) does not apply; a genuine four-quark theory would be required. However, the source terms corresponding to those on the right of (4.6c) in such a theory are also small at this stage because the d and d wave functions are perturbations. Therefore, the condition corresponding to (6.1) holds at this stage.

The initial stage is followed by the intermediary stage of Fig. 1b. In Fig. 1 of III for $D^{*0} \to D^0\gamma$, the c and $\bar{u}$ quarks move inward and one of them flips its spin to form a D^0, the energy released goes to the photon and D^0. Analogously, the c and $\bar{u}$ quarks in Fig. 1a behave in the same way to form a D^0, the energy released now goes, in addition to D^0, also to create a distance between the d and d quarks in Fig. 1a and converts this virtual pair into a real meson in the end. In this intermediary stage, x_{III} (x_I) is considered to be close enough to $x_{IV}(x_{II})$ so that the approximation (4.1) applies.

In this stage, both embryo pseudoscalar mesons interact strongly with each other and the meson wave functions are not uniformly distributed in **X** space. This stage is too complex to allow for an estimate of the source wave functions. It is not known whether (6.1) is violated or not. However, the effect of an eventual violation is small because this stage lasts a very short time compared to the duration of the final stage below, so that its contribution to the time integral of (5.6) is small.

Since diquarks do not exist, c and d tend to move away from each other. This leads to the final stage, depicted in Fig 1c. Both pseudoscalar mesons D^0 and dd are moving away from each other. The same process holds for $dd \to \bar{u}u$ and a π^0 is observed (see note a in Table 4 of ref. 9). After a short time, small compared to the decay time T_d in (7.2), the so-produced pseudoscalar mesons have moved so far away from each other that they no longer interact with each other via strong forces and can hence be considered as free mesons.

The absolute magnitude of their amplitudes according to (2.2a) and (2.3a) is proportinal to $1/\sqrt{\Omega} \to 0$, so that (4.6c) is small and (6.1) holds. But in this stage the quarks $\bar{u}$ (c) and d (d) are so far apart that (4.1) and hence (4.6c) are no longer valid. Nevertheless, it is possible to set

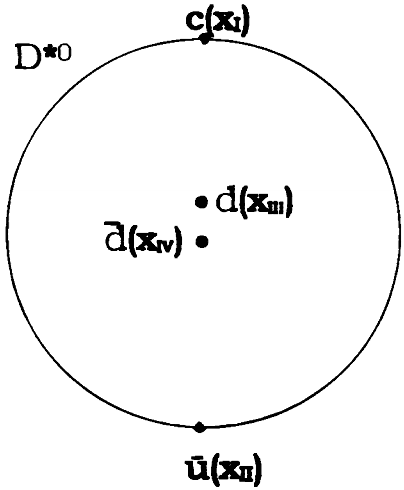

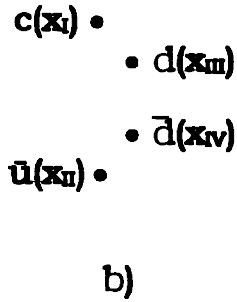

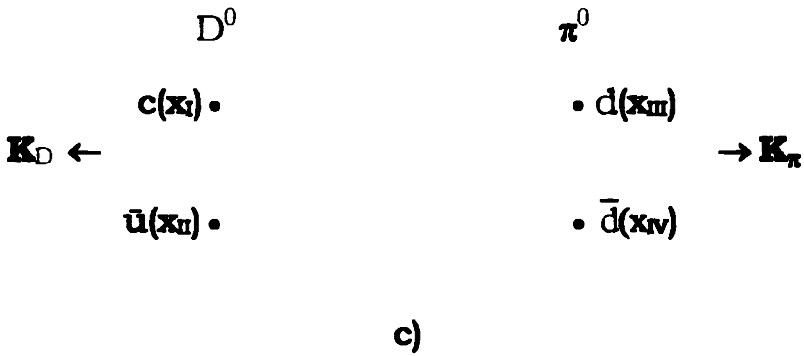

Fig. 1. Illustration of $D^{*0} \to D^0\pi^0$. (a) In the initial stage the peak of the free D^{*0} amplitude is located on the circle according to (2.6b) and a virtual pair dd with small amplitude is created at the origin. The c and $\bar{u}$ quarks tend to lower their energy in the potential well $-d_m/r$ of (2.1b) by moving toward each other to form the final state pseudoscalar meson D^0, which has a much smaller radius and hence much lower potential energy. (b) In the intermediary stage the c and $\bar{u}$ quarks have moved inward and the potential energy released goes to compensate for the energy needed to create a separation of d from $\bar{d}$ in order to form a quasi-dd pseudoscalar meson. The spin of c or $\bar{u}$ flips to convert D^{*0} to D^0. Also, the quarks $\bar{u}(c)$ and $d(\bar{d})$ start to move away from each other since the diquark does not exist. With $dd \to \bar{u}u$ in half of the time, it becomes a π^0. This process continues until it reaches the final stage (c), in which D^0 and π^0 become free mesons.

$$X^3 = \tfrac{1}{2}(x_{\mathrm{I}}^3 + x_{\mathrm{II}}^3) = -\tfrac{1}{2}(x_{\mathrm{III}}^3 + x_{\mathrm{IV}}^3), \qquad X^0 = \tfrac{1}{2}(x_{\mathrm{I}}^0 + x_{\mathrm{II}}^0) = \tfrac{1}{2}(x_{\mathrm{III}}^0 + x_{\mathrm{IV}}^0)$$
$$\bar{x} = \bar{x}_{\mathrm{II}} - \bar{x}_{\mathrm{I}} = \bar{x}_{\mathrm{IV}} - \bar{x}_{\mathrm{III}} \tag{6.2}$$

where the superscript 3 denotes the direction of the meson velocity. This is possible because of (i) the symmetry in the motions of the quarks in both mesons, (ii) the flavor independence of nonrelativistic free meson wave functions, and (iii) the fact that the wave functions are finally integrated over **x** and **X** in (5.6).

The spin of the D^{*0} is transferred to a relative angular momentum between both pseudoscalar mesons. Formally, this can be seen by applying (III 3.6) to the upper integrand of (5.6) to obtain

$$\psi_{\mathrm{I}}(r) \lfloor 2\hat{r}\, \Phi_{1P4}(\exp(iE_{\mathrm{I}0} X^0)) \rfloor \hat{r}\, \psi_{\mathrm{I}}(r)$$

Here, the last $\hat{r}$ represents the vector character of the initial state and the first $\hat{r}$ denotes the spin state of the both pseudoscalar mesons, represented by the bracket using (6.5) and (6.9) below.

6.2. Perturbed Potential

The negative-energy solutions for the pseudoscalar meson *CB* in motion are chosen in (4.6c). The terms on the right of (4.6c) that will contribute in the final stage (Fig. 1c) are written as

$$-\frac{1}{16}(\psi_{AB}^{a\dot{b}} \chi_{CD}^{*\dot{b}a} + \psi_{CD}^{*a\dot{b}} \chi_{AD\dot{b}a})$$
$$-\frac{1}{16}\exp[i(\bar{\bar{K}}_{0AD} - \bar{\bar{K}}_{0CB})\bar{\bar{X}} - i(E_{0\bar{K}AD} + E_{0\bar{K}CB})X^0]$$
$$\times 2(\psi_{0\bar{K}AD}(\bar{\bar{x}})\chi_{0\bar{K}CB}^{*}(\bar{\bar{x}}) - \bar{\psi}_{0\bar{K}AD}(\bar{\bar{x}})\bar{\chi}_{0\bar{K}CB}^{*}(\bar{\bar{x}}) + \psi \leftrightarrow \chi) \tag{6.3}$$

where the form of (III 3.1) with $b_{J\mathbf{K}} = 1$ has been employed. Comparison of (5.4b) to (5.6) together with (4.6c) and (6.3) shows that

$$\bar{\bar{K}}_{0AD} = \bar{\bar{K}}_{0CB} = \bar{\bar{K}}_0 \tag{6.4}$$

Replacing the right of (4.6c) by (6.3) and using (III A3) with $a = 1/2$ given above (III 4.2) leads to the form

$$\Phi_{1P4}(x_{\mathrm{I}}, x_{\mathrm{II}}) = \Phi_{1P}(\bar{\bar{x}}) \exp[i(\bar{\bar{K}}_{0AD} - \bar{\bar{K}}_{0CB})\bar{\bar{X}} - i(E_{0\bar{K}AD} + E_{0\bar{K}CB})X^0] \tag{6.5}$$

Using this expression, the left of (4.6c) similarly becomes

$$\{\exp[i(\bar{\bar{K}}_{0AD} - \bar{\bar{K}}_{0CB})\bar{\bar{X}} - iE_{10}X^0]\}\left(\nabla^2 + \frac{E_{10}^2}{4}\right)^2 \Phi_{1P}(\bar{\bar{x}}) \tag{6.6a}$$

$$E_{10} = E_{0\bar{\bar{K}}AD} + E_{0\bar{\bar{K}}CB} \tag{6.6b}$$

The last relation is evident from (5.4b), (5.6) and (6.5).

6.3. Green's Functions

Equating (6.6a) to (6.3) yields

$$\left(\nabla^2 + \frac{E_{10}^2}{4}\right)^2 \Phi_{1P}(\bar{\bar{x}}) = -\frac{1}{8}\begin{pmatrix}\psi_{0\bar{\bar{K}}AD}(\bar{\bar{x}})\chi^*_{0\bar{\bar{K}}CB}(\bar{\bar{x}}) - \bar{\psi}_{0\bar{\bar{K}}AD}(\bar{\bar{x}})\bar{\chi}^*_{0\bar{\bar{K}}CB}(\bar{\bar{x}}) + \\ \chi^*_{0\bar{\bar{K}}AD}(\bar{\bar{x}})\psi_{0\bar{\bar{K}}CB}(\bar{\bar{x}}) - \chi^*_{0\bar{\bar{K}}AD}(\bar{\bar{x}})\bar{\psi}_{0\bar{\bar{K}}CB}(\bar{\bar{x}})\end{pmatrix} \tag{6.7}$$

The Green's function for (6.7) satisfies

$$\left(\nabla^2 + \frac{E_{10}^2}{4}\right)^2 G(\bar{\bar{x}}, \bar{\bar{x}}') = \delta(\bar{\bar{x}} - \bar{\bar{x}}') \tag{6.8a}$$

$$G(\bar{\bar{x}}, \bar{\bar{x}}') = -\frac{1}{4\pi E_{10}} \sin\left(\frac{1}{2} E_{10}|\bar{\bar{x}} - \bar{\bar{x}}'|\right) \tag{6.8b}$$

In the $E_{10} \to 0$ limit, (6.8b) reduces to

$$G(\bar{\bar{x}}, \bar{\bar{x}}') = -|\bar{\bar{x}} - \bar{\bar{x}}'|/8\pi \tag{6.8c}$$

which is the confining Green's function of (I 7.1) for the zeroth-order Φ_{PAB} of (4.6b). Note that homogeneous solutions of the type $1/|\mathbf{x} - \mathbf{x}'|$ and constant that accompany (6.8c), as in (I 7.2), cannot be added to (6.8b) due to the presence of E_{10}. Applying (6.8a) and (6.8b) to (6.7) yields

$$\begin{aligned} I_{1P}(\bar{\bar{x}}) &= 8\pi E_{10}\Phi_{1P}(\bar{\bar{x}}) \\ &= \frac{1}{4}\int d^3\bar{\bar{x}}' \begin{bmatrix}\psi_{0\bar{\bar{K}}AD}(\bar{\bar{x}}')\chi^*_{0\bar{\bar{K}}CB}(\bar{\bar{x}}') - \bar{\psi}_{0\bar{\bar{K}}AD}(\bar{\bar{x}}')\bar{\chi}^*_{0\bar{\bar{K}}CB}(\bar{\bar{x}}') + \\ \chi^*_{0\bar{\bar{K}}AD}(\bar{\bar{x}}')\psi_{0\bar{\bar{K}}CB}(\bar{\bar{x}}') - \chi^*_{0\bar{\bar{K}}AD}(\bar{\bar{x}}')\bar{\psi}_{0\bar{\bar{K}}CB}(\bar{\bar{x}}')\end{bmatrix} \\ &\quad \sin\left(\frac{1}{2} E_{10}|\bar{\bar{x}} - \bar{\bar{x}}'|\right) \end{aligned} \tag{6.9}$$

For nonrelativistic mesons, vector product terms in (6.9) are of order ϵ_0^2 and can be dropped. The bracket in (6.9) then depends only upon $|\mathbf{x}'| = r'$ and angular integrations can be carried out to yield

$$I_{1P}(r) = \frac{8\pi}{E_{10}^3}\left\{\begin{array}{l} \dfrac{\cos R}{R}\displaystyle\int_0^R dR'\ R'(\sin R' - R'\cos R')\,[\ldots(r')] + \\ \sin R\displaystyle\int_0^R dR'\ R'[\ldots(r')]\sin R' - \\ \cos R\displaystyle\int_R^\infty dR'\ R'[\ldots(r')]\cos R' + \\ \dfrac{\sin R}{R}\displaystyle\int_R^\infty dR'\ R'(\cos R' + R'\sin R')[\ldots(r')] \end{array}\right\} \tag{6.10a}$$

$$R = E_{10}r/2, \qquad [\ldots(r')] = [\ldots] \text{ in (6.9)} \tag{6.10b}$$

In the $E_{10} \to 0$ limit, $\sin(E_{10}|\mathbf{x} - \mathbf{x}'|/2) \to E_{10}|\mathbf{x} - \mathbf{x}'|/2$ and (6.9) takes the form of (I 7.2) for the zeroth-order potential Φ_{PAB}. In that limit, (6.10) reduces to the form of the bracket in (I 7.4) or (3d) of ref. 9 times $E_{10}/2$ for the confining potential.

7. DECAY RATE

Inserting (6.9) and (6.5) into (5.6) and performing the X^0 integration yields

$$S_{fi} = \frac{-i}{E_{10}^2\Omega_N}\int d^3\bar{\bar{X}}\ (\exp\, i(\bar{\bar{K}}_{0AD} - \bar{\bar{K}}_{0CB})\bar{\bar{X}})\delta(E_{10} - E_{0\bar{\bar{K}}AD} - E_{0\bar{\bar{K}}CB})$$
$$\times \int d^3\bar{\bar{x}}\ \psi_1^2(r)\ \mathrm{Re}\ I_{1P}(\bar{\bar{x}}) \Big/ \int d^3\bar{\bar{x}}\ \psi_1^2(r) \tag{7.1}$$

Here, (III 3.6) has been used. The decay rate corresponding to (III 4.3) is

$$\Gamma(\mathrm{V} \to \mathrm{PP}) = \sum_{\text{final states}} |S_{fi}|^2/T_d = \frac{\Omega_N^2}{64\pi^6}\int d^3\bar{\bar{K}}_{0AD}\int d^3\bar{\bar{K}}_{0CB}\ |S_{fi}|^2/T_d \tag{7.2}$$

Inserting (7.1) into (7.2) and carrying out the $\mathbf{X}$ integration in a manner analogous to that leading to (III 4.3) gives

$$\Gamma(\mathrm{V} \to \mathrm{PP}) = \frac{1}{4\pi^3}\frac{\Omega_d}{\Omega_N^2}(\Omega_N\bar{I}_{1P})^2 C_g^2 P_K \tag{7.3a}$$

$$\Omega_d = \int d^3\bar{\bar{X}}\ (\exp\, i(\bar{\bar{K}}_{0AD} - \bar{\bar{K}}_{0CB})\bar{\bar{X}}) = 8\pi^3\delta(\bar{\bar{K}}_{0AD} - \bar{\bar{K}}_{0CB}) = (2\pi\delta(0))^3 \tag{7.3b}$$

$$P_K = E_{10}^{-5} K_0 \sqrt{E_{00AD}^2 + K_0^2}\,\sqrt{E_{00CB}^2 + K_0^2}, \qquad K_0 = \sqrt{\lambda}/2E_{10} \tag{7.3c}$$

$$\lambda = E_{10}^4 + E_{00AD}^4 + E_{00CB}^4 - 2E_{10}^2(E_{00AD}^2 + E_{00CB}^2) - 2E_{00AD}^2 E_{00CB}^2 \tag{7.3d}$$

$$\bar{I}_{1P} = \int d^3\bar{x}\ \psi_1^2(r)\ \mathrm{Re}\ I_{1P}(\bar{x}) \Big/ \int d^3\bar{x}\ \psi_1^2(r) \tag{7.4}$$

where $K_0 = |\mathbf{K}_0|$ of (6.4). Since the decay is strong, the branching ratio determined by the isospin Clebsch–Gordan coefficient C_g has been inserted.

The E_{00} are the masses of the pseudoscalar mesons AD and CB determined by (2.1e). The relation (III B10), shown to hold to order ε_0, has been used in deriving (7.3c), (7.3d).

As was mentioned in Section 6.1 in connection with Fig. 1b, the time during which the four quarks are close together is short compared to the decay time T_d. During the greater part of T_d, the mesons have moved so far from each other that they behave like free mesons. Limiting consideration to nonrelativistic mesons or $\varepsilon_0 \ll 1$, as in (III B5), they can be described by the rest-frame free meson wave function (2.2a) and (2.3a), putting Ω to Ω_N by (5.4a). Inserting these expressions into (7.4) using (6.9) and (2.2b) leads to

$$\Omega_N \bar{I}_{1P} = g_q^4(1 + \Delta_2) I_{VP} \tag{7.5a}$$

$$\begin{aligned} I_{VP} &= -\frac{d_m^3}{16} \int d^3\bar{x}\ r^2 \exp\left(\frac{-d_m r}{2}\right) \int d^3\bar{x}'\ \sin\left(\frac{1}{2} E_{10} |\bar{x} - \bar{x}'|\right) \\ &\quad \times \exp(-d_m r') \Big/ \int d^3\bar{x}\ r^2 \exp\left(\frac{-d_m r}{2}\right) \\ &= \frac{1}{4}\left(\frac{b}{1 + 4b^2}\right)^3 \left[\frac{16}{243}(1 + 10b^2) - \frac{32b^6}{(1 + b^2)^5}\right. \\ &\quad \left. \times (2 - 11b^2 - 40b^4 + 21b^6)\right], \qquad b = \frac{d_m}{E_{10}} \end{aligned} \tag{7.5b}$$

where (6.10) has been employed.

The g_q^2 factors in (A3) have been absorbed into the meson wave function by (A5a) or (I 6.11) so that they are not visible in (A9). This scale change makes no difference in linear problems, but plays an essential role in the nonlinear problem here. Therefore, this g_q^2 factor is reinstated so that g_q^4 is multiplied into the right of (A9) so that it takes the original form (I 4.12). This g_q^4 factor now appears in (7.5a).

The Δ_2 in (7.5a) represents the ε_0^2 terms in (6.9). This relativistic correction term cannot be evaluated because (III B8)–(III B9) have not been solved.

Its order of magnitude has, however, been estimated using dimensional analysis and is given by (III B14) and (III B17) in the heavy meson limit. In this approximation, no new integrals are involved and

$$\Delta_2 = K_0^2\left(\frac{1}{E_{00\,AD}E_{00\,CB}} - \frac{8}{d_m}\right), \qquad \varepsilon_0 \ll 1, \quad d_m \ll E_{00} \tag{7.6}$$

The infrared cutoffs Ω_d and Ω_N^2 are also not known, but

$$\Omega_d/\Omega_N^2 = M_{ds}^3 \tag{7.7}$$

must be some finite constant to obtain a finite decay rate, just like in the weak decay case (3.14). Such ratios of two large quantities, each approaching infinity, are a particular feature of the spinor strong interaction theory and their roles are not understood presently.

The decay rate (7.3a) now becomes

$$\Gamma(\mathrm{V} \to \mathrm{PP}) = C_1 C_g^2 P_k I_{VP}^2 (1 + \Delta_2)^2, \qquad C_1 = g_q^8 M_{ds}^3/4\pi^3 \tag{7.8}$$

which together with (7.3c), (7.3d) and (7.5b) determines the decay rate for nonrelativistic decay products.

8. APPLICATION AND COMPARISON TO EARLIER WORK

8.1. V $\to$ PP Decay Rates

The decay rate (7.8) can now be applied to the various decays in Table I. It holds for $\varepsilon_0 \ll 1$, so that $\Delta_2 \ll 1$ and can be neglected. The condition for the estimate of Δ_2 by (7.6) is not met by the decays in Table I except for D*. The predicted decay rates are obtained by putting Δ_2 to 0. Futher, C_1 in (7.8) is fixed by the measured $\Gamma(\varphi \to \mathrm{K}^+\mathrm{K}^-)$ and is $C_1 = 0.35\ \mathrm{GeV}^3$. Since ε_0 is not very small according to Table I, the Δ_2 term for this decay may cause an error of 10–20% in this C_1 value.

For D*, $\varepsilon_0 \ll 1$, so that the predictions are expected to hold rather well. Since (7.6) holds for this decay, it reduces the rates by 2–2.6%. Data [1] show that $\Gamma(\mathrm{D}^{*+} \to \mathrm{D}^0\pi^+)/\Gamma(\mathrm{D}^{*+} \to \mathrm{D}^+\pi^0) = 2.23 \pm 0.28$. This value is 11.6% greater than the ratio 2 obtained from the Clebsch–Gordan coefficients. In Table I this ratio 2 is raised to 2.13, within experimental error. The very small decay rates are due to the canceling effect of the sine factor in (7.5b) and are far below the measured upper limits. An experimental determination of these rates can provide an important test for the spinor strong interaction theory.

For K* and ρ, ε_0 is no longer small and the Δ_2 term will be appreciable. Nevertheless, the predicted values are off only by a factor of about 2 and support qualitatively the present approach to strong decays.

Table I. Decay Rates and Parameters Limiting Their Validity Regions[a]

	$\varepsilon_0 = K_0/E_{00}$	ε_0^2	C_g^2	Γ (keV) (7.8)	Γ (keV) Data[1]
$D^{*+} \to D^+\pi^0$	0.021 (D) 0.284 (π)	0.00596	1/3	0.012	<40
$D^{*+} \to D^0\pi^+$	0.021 (D) 0.284 (π)	0.00596	2/3	0.025	<89.5
$D^{*0} \to D^0\pi^0$	0.023 (D) 0.32 (π)	0.00736	1/3	0.013	<1300
$D^{*0} \to D^+\pi^-$	0.023 (D) 0.32 (π)	0.00736	2/3	0	0
$\varphi \to K^+K^-$	0.257	0.066	1/2	Input	2.18×10^3
$\varphi \to \bar{K}^0K^0$	0.221	0.0488	1/2	1.89×10^3	1.51×10^3
$K^{*+} \to K^+\pi^0$	0.586 (K) 2.14 (π)	1.26	1/3		
				25.2×10^3	49.8×10^3
$K^{*+} \to K^0\pi^+$	0.574 (K) 2.05 (π)	1.17	2/3		
$K^{*0} \to K^0\pi^0$	0.583 (K) 2.15 (π)	1.25	2/3		
				24.8×10^3	50.5×10^3
$K^{*0} \to K^+\pi^-$	0.59 (K) 2.09 (π)	1.23	1/3		
$\rho^+ \to \pi^+\pi^0$	≈ 2.6	6.91	1		
				62.5×10^3	151×10^3
$\rho^0 \to \pi^+\pi^-$	2.61	6.81	1		

[a] Column 2 gives the relative momenta of the decay products. Column 3 shows the product of the ε_0's in column 2 for both decay products and is a measure of Δ_2 in (7.8). The isospin Clebsch–Gordan coefficient factor in (7.8) is given in column 4 and the data [1] in column 6. The decay rates in column 5 are obtained from (7.8) with (7.5b), (7.3c), and (7.3d), putting $\Delta_2 = 0$, and hold only for $\varepsilon_0 \ll 1$. For K* and ρ, $\varepsilon_0 \gg 1$ and $\Delta_2 \neq 0$, so that the decay rates are only estimates.

8.2. Ratios of $V \to P\gamma$ and $V \to P\pi^0$ Decay Rates

The results in Table I may be combined with the order-of-magnitude estimates of the radiative decay rates in Table 1 of III. Some results are shown in Table II.

The estimated ratios are consistent with the measured ones, given that $\Gamma(V \to P\gamma)$ is an order-of-magnitude estimate and that $\Gamma(V \to P\pi^0)$ is also an estimate due to the unknown Δ_2, except for D*. The too large estimates for ρ stem from the too large $\Gamma(\rho \to \pi\gamma)$ in Table I of III and are discussed at the end of Section 5.1 of III. On the other hand, the order-of-magnitude agreement for the D* case is rather remarkable in view of the very small

Table II. Ratios of Radiative and Strong Decay Rates[a]

	$\frac{\Gamma(D^{*0} \to D^0\gamma)}{\Gamma(D^{*0} \to D^0\pi^0)}$	$\frac{\Gamma(D^{*+} \to D^+\gamma)}{\Gamma(D^{*+} \to D^+\pi^0)}$	$\frac{\Gamma(K^{*0} \to K^0\gamma)}{\Gamma(K^{*0} \to K^0\pi^0)}$	$\frac{\Gamma(K^{*+} \to K^+\gamma)}{\Gamma(K^{*+} \to K^+\pi^0)}$	$\frac{\Gamma(\rho^+ \to \pi^+\gamma)}{\Gamma(\rho^+ \to \pi^+\pi^0)}$
Estimate	0.21	0.015	3.23×10^{-3}	$\geq 1.72 \times 10^{-3}$ $< 17.2 \times 10^{-3}$	$> 2.2 \times 10^{-3}$ $\leq 22 \times 10^{-3}$
Data [1]	0.615	0.036	3.45×10^{-3}	3.03×10^{-3}	0.9×10^{-3}

[a] The estimated values are ratios of the order-of-magnitude estimates of $\Gamma(V \to P\gamma)$ of Table I in III to the predicted Γ in Table I here. The last line gives the experimental data, using the Clebsch–Gordan coefficients in Table I.

$\Gamma(D^*)$ values in Table I and of the rather coarse estimate of (4.8) and (4.10a) of III.

8.3. Comparison to Earlier Work

The present work differs basically from earlier ones [3–6] which were based upon phenomenological Lagrangians (not derivable from first-principle theories such as QCD). These consist of local meson fields and the physics related to the finite size of the mesons is largely lost. These Lagrangians have been constructed for different applications, are different from each other, and often contain a large number of terms and many free parameters to be fixed by nearly as many data points. They cannot account for more general mesonic phenomena such as confinement, meson spectra, the U(1) problem, the absence of Higgs bosons, etc.

The chiral perturbation theories and the decay rates obtained from them hold approximatively for light mesons [3, 4]. When the meson contains a quark with mass $\to \infty$, a new spin-flavor symmetry appears in QCD [5]. $\Gamma(D^{*+} \to D^0\pi^+)$ has been estimated in this heavy quark symmetry limit [6]. However, correction due to the finite c quark mass, which can be appreciable, has not been included and the predicted rates depend upon the data chosen to fix the parameters.

In contrast, the Lagrangian in (5.1) is Lorentz and gauge invariant. It is nonlocal, contains the internal structure of the mesons, and is much simpler than the phenomenological Lagrangians. The same Lagrangian also led to predictions on confinement (I), meson spectra [9], the U(1) problem [8], the absence of Higgs bosons [8], weak decay (II), and radiative decay (III), if appropriate gauge fields are incorporated.

In the nonrelativistic limit, $\Delta_2 = 0$ in (7.8). The only free parameter is C_1, which is fixed by $\Gamma(\varphi \to K^+K^-)$. The fundamental mesonic length $1/d_m$ in (2.5a) was determined in I.

9. POSSIBLE CONNECTION OF STRONG TO ELECTROMAGNETIC INTERACTIONS AND FORMAL DECOUPLING OF ELECTROMAGNETIC AND WEAK INTERACTIONS

9.1. Possible Connection of Strong and Electromagnetic Interactions

The radiative and strong decay rates of D* in Table II are of the same order of magnitude. The phase spaces available for both types of decay are very small due to the small difference of D* and D masses. Next to D, π^0 and γ are both light particles. These observations may indicate that both types of decay are associated with the same coupling strength.

This can also be seen from the similarity between Fig. 1 of III and Fig. 1 here. As was discussed in Section 6.1, the initial stage of both decays is the same, i.e., the inward motion of both quarks in the vector meson. A photon is emitted in the radiative decay, but is reabsorbed by a virtual $\bar{q}q$ pair to form a real $\bar{q}q$ meson to be emitted in the corresponding strong decay.

Each type of decay is characterized by its coupling strength. The coupling strength of the weak decay rate (II 6.5) or (3.13) is determined by the Fermi coupling constant

$$G = \sqrt{2}\, g^2/8M_W^2 \tag{9.1}$$

according (II 6.4), where M_W is the gauge boson mass and g the weak charge. The coupling strength of the electromagnetic or radiative decay rate (III 4.3) is the fine structure constant α in form of the square of the quark charges. The coupling strength of the strong decay rate (7.8) is g_q^8. The M_{ds}^3 factor there, given by (7.7), is of basic importance in strong decay, but is not related to the quark–quark coupling constant g_q^2 in (A3).

Therefore, it may be conjectured that the strong and electromagnetic couplings are connected to each other by relating the strong meson–meson coupling constant g_q^8 in (7.8) to the electromagnetic one, the fine structure constant α, in the radiative decay rate (III 4.3) according to

$$(g_q^2/4\pi)^4 \equiv \alpha_s^4 = \alpha \equiv e^2/4\pi \cong 1/137 \tag{9.2a}$$

$$\alpha_s = (\pm 1, \pm i) \times 0.2923 \tag{9.2b}$$

$$g_q = (\pm 1, \pm i, \pm(1 \pm i)/\sqrt{2}) = 6.328e \tag{9.3}$$

A factor of $1/(4\pi)^3$ has been absorbed into the $M_{ds}^3/4\pi^3$ factor in C_1 in (7.8). It is seen that α_s is of the same magnitude that appears in the literature, but can be imaginary here. The hypothesis (9.2) may eliminate one more "fundamental parameter" α_s, in the literature [1], in addition to the Cabbibo angle (II 11.4) in the meson sector and the Weinberg angle [see (9.5) ff.] in the limit of SU(3) flavor symmnetry. Such a connection (9.3) has in addition

the cosequence that the existence of the electron implies that the quark or hadron also exists.

9.2. Detachment of Electromagnetic and Weak Couplings

Independent of the above connection in Section 9.1, such a detachment is already implicit in Section 3.4, which will be made explicit here. In the standard electroweak model [1], the strength of the weak processes is controlled by the Fermi constant (9.1), where the weak charge g is related to the electron charge $-e$ via the Weinberg angle,

$$\sin \vartheta_w = e/g \cong 1/2 \tag{9.4}$$

which in effect couples the electromagnetic and weak interactions.

In the spinor strong interaction theory, however, G is independent of g, hence also e, according to (9.1) and (3.10):

$$G = 1/\pi \sqrt{2\pi} N_{c00} \tau_0 = 2 \sqrt{2/\pi} \Omega/\tau_0 \tag{9.5}$$

The last relation is obtained from (2.1d), (2.2a), and (2.3a) and shows that the Fermi constant is the ratio of two large parameters, each $\to\infty$, but at different rates, just like M_{ds} in (3.14) and M_{dW} in (7.7) do.

Further, the Weinberg angle in (9.4) has, in the limit of SU(3) flavor symmetry, its origin in the $1/\sqrt{3}$ factor in the eighth of the Gell-Mann matrices according to (5.2) and what follows in ref. 11. Thus, (9.4) is related to the nomalization of the Gell-Mann matrices and not to any physical coupling of electromagnetic and weak interactions. From this viewpoint, the Fermi constant in weak interactions is dissociated from electromagnetic interactions.

Such a detachment is not possible in the standard model because M_W in (9.1) is a constant generated by the hypothetical Higgs boson which is unrelated to g. Since no Higgs boson has been found after decades of search, the standard model is probably incorrect in this basic aspect. In the spinor strong interaction theory, the low-lying pseudoscalar meson doublet and triplet play the role of the Higgs boson [8, II] and no such difficulty exsists. As was shown in II, the remaining main results of the standard model can be taken over and are not affected by this decoupling.

That the strong and electromagnetic couplings are interconnected while the electromagnetic and weak couplings are disconnected is more natural than the current view in which the connection and disconnection are reversed. The electromagnetic and strong interactions both conserve parity, while weak interactions violate maximally parity conservation. Further, α is smaller than α_s by a factor of about 40 according to (9.2), but is greater than the weak coupling constant Gm_μ^2 by a factor of about 10^5.

APPENDIX. CONSTRUCTION OF TWO-QUARK MESON WAVE EQUATIONS

Construction of two-quark meson wave equations (I 5.4) and (I 4.12) has been carried out in Sections 4 and 5 of I. This is repeated here to facilitate the construction of the four-quark meson wave equations in Section 2. Some errors in Section 4 of I, which do not affect the meson equations there, are removed here.

Equations for a quark A and an antiquark B under mutual pseudoscalar interaction (I 5.1), (I 5.2), and (I 4.7) read

$$\partial_{\mathrm{I}}^{ab}\chi_{Ab}(x_{\mathrm{I}})\xi_A^p(z_{\mathrm{I}}) = i(m_{Aop}(z_{\mathrm{I}}, \partial/\partial z_{\mathrm{I}}) - V_{PB}(x_{\mathrm{I}}))\psi_A^a(x_{\mathrm{I}})\xi_A^p(z_{\mathrm{I}}) \tag{A1a}$$

$$\partial_{I\dot{c}b}\psi_A^b(x_{\mathrm{I}})\xi_A^p(z_{\mathrm{I}}) = i(m_{Aop}(z_{\mathrm{I}}, \partial/\partial z_{\mathrm{I}}) + V_{PB}(x_{\mathrm{I}}))\chi_{A\dot{c}}(x_{\mathrm{I}})\xi_A^p(z_{\mathrm{I}}) \tag{A1b}$$

$$\partial_{\mathrm{II}\dot{e}f}\chi_B^f(x_{\mathrm{II}})\xi_{Br}(z_{\mathrm{II}}) = i(m_{Bop}(z_{\mathrm{II}}, \partial/\partial z_{\mathrm{II}}) - V_{PA}(x_{\mathrm{II}}))\psi_{B\dot{e}}(x_{\mathrm{II}})\xi_{Br}(z_{\mathrm{II}}) \tag{A2a}$$

$$\partial_{\mathrm{II}}^{d\dot{e}}\psi_{B\dot{e}}(x_{\mathrm{II}})\xi_{Br}(z_{\mathrm{II}}) = i(m_{Bop}(z_{\mathrm{II}}, \partial/\partial z_{\mathrm{II}}) + V_{PA}(x_{\mathrm{II}}))\chi_B^d(x_{\mathrm{II}})\xi_{Br}(z_{\mathrm{II}}) \tag{A2b}$$

$$\Box_{\mathrm{I}} V_{PB}(x_{\mathrm{I}}) = \frac{i}{2} g_q^2[\psi_B^b(x_{\mathrm{I}})\chi_{Bb}(x_{\mathrm{I}}) - \text{c.c.}] \tag{A3a}$$

$$\Box_{\mathrm{II}} V_{PA}(x_{\mathrm{II}}) = \frac{i}{2} g_q^2[\psi_A^a(x_{\mathrm{II}})\chi_{Ad}(x_{\mathrm{II}}) - \text{c.c.}] \tag{A3b}$$

where $\chi_B^d = (\chi_B^{\dot{d}})^*$. In (I 4.7), let

$$g_A g_B \to g_q^2 \tag{A3c}$$

Similarly, the g's in (2.4) and (2.7) of ref. 15 for scalar strong interaction among quarks are also identified as g_q; there is no reason why pseudoscalar and scalar strong quark–quark coupling should be different.

Since (A3) cannot contain any function of the internal coordinate z, the wave function $\psi\xi$ in (A1) and (A2) has been multiplied by ξ^* to yield $\xi^*\psi\xi = \psi$ by using the reverse of (A6a) below, (III A9), and (III A5b).

Now multiply together (A1a) and (A2a):

$$\begin{aligned}\partial_{\mathrm{I}}^{of}\partial_{\mathrm{II}\dot{e}f}\chi_{Ao}(x_{\mathrm{I}})\chi_B^f(x_{\mathrm{II}})\xi_A^p(z_{\mathrm{I}})\xi_{Br}(z_{\mathrm{II}}) \\ = -(m_{Aop}m_{Bop} + V_{PA}(x_{\mathrm{II}})V_{PB}(x_{\mathrm{I}}) - m_{Aop}V_{PA}(x_{\mathrm{II}}) \\ - m_{Bop}V_{PB}(x_{\mathrm{I}}))\psi_A^a(x_{\mathrm{I}})\psi_{B\dot{e}}(x_{\mathrm{II}})\xi_A^p(z_{\mathrm{I}})\xi_{Br}(z_{\mathrm{II}})\end{aligned} \tag{A4}$$

The basic hypothesis of the spinor strong interaction theory for mesons consists in the following generalizations. In the first place, the products of quark and antiquark wave functions are generalized into nonseparable meson wave functions according to

$$g_q^2 \chi_{Ab}(x_\mathrm{I}) \chi^f_B(x_\mathrm{II}) \rightarrow \chi^f_b(x_\mathrm{I}, x_\mathrm{II}), \qquad g_q^2 \psi^a_A(x_\mathrm{I}) \psi_{B\dot{e}}(x_\mathrm{II}) \rightarrow \psi^a_{\dot{e}}(x_\mathrm{I}, x_\mathrm{II}) \tag{A5a}$$

Next, the product of the pseudoscalar potentials for the quark A and antiquark B is analogously generalized into a nonseparable meson potential according to

$$V_{PA}(x_\mathrm{II}) V_{PB}(x_\mathrm{I}) \rightarrow -\Phi_p(x_\mathrm{I}, x_\mathrm{II}) \tag{A5b}$$

Consistent with these generalizations in space-time, the corresponding generalizations in internal space are made:

$$\xi^p_A(z_\mathrm{I}) \xi_{Br}(z_\mathrm{II}) \rightarrow \xi^p_r(z_\mathrm{I}, z_\mathrm{II}) \tag{A6a}$$

$$m_{Aop}(z_\mathrm{I}, \partial/\partial z_\mathrm{I}) m_{Bop}(z_\mathrm{II}, \partial/\partial z_\mathrm{II}) \rightarrow m_{2op}(z_\mathrm{I}, \partial/\partial z_\mathrm{I}, z_\mathrm{II}, \partial/\partial z_\mathrm{II}) \tag{A6b}$$

Insert (A5) and (A6) into (A4). Since the quarks are not observable, their wave functions are put to zero. Therefore, $\mathrm{V}_{PA} = \mathrm{V}_{PB} = 0$ also by (A3). Equation (A4) now becomes

$$\partial^{ab}_\mathrm{I} \partial_{\mathrm{II}\dot{e}f} \chi^f_b(x_\mathrm{I}, x_\mathrm{II}) \xi^p_r(z_\mathrm{I}, z_\mathrm{II}) = (\Phi_P(x_\mathrm{I}, x_\mathrm{II}) - M_m^2) \psi^a_{\dot{e}}(x_\mathrm{I}, x_\mathrm{II}) \xi^p_r(z_\mathrm{I}, z_\mathrm{II}) \tag{A7a}$$

$$m_{2op}(z_\mathrm{I}, \partial/\partial z_\mathrm{I}, z_\mathrm{II}, \partial/\partial z_\mathrm{II}) \xi^p_r(z_\mathrm{I}, z_\mathrm{II})$$

$$= \left[\sum_\nu \frac{m_\nu}{2} \left(z^\nu_\mathrm{I} \frac{\partial}{\partial z^\nu_\mathrm{I}} + z^\nu_\mathrm{II} \frac{\partial}{\partial z^\nu_\mathrm{II}} \right) + \text{c.c.} \right]^2 \xi^p_r(z_\mathrm{I}, z_\mathrm{II}) = M_m^2 \xi^p_r(z_\mathrm{I}, z_\mathrm{II}) \tag{A7b}$$

The internal wave function ξ^p_r characterizes its flavor content via the quark flavors p and r and has been given by (III A9). m_{2op} of (A7b) is of the form (I 9.6a) and m_ν is the quark mass of flavor ν so that

$$M_m = \tfrac{1}{2}(m_p + m_r) \tag{A7c}$$

Multiplying together (A1b) and (A2b) and following the same procedure leads analogously to

$$\partial_{\mathrm{I}c b} \partial^{d\dot{e}}_\mathrm{II} \psi^b_{\dot{e}}(x_\mathrm{I}, x_\mathrm{II}) \xi^p_r(z_\mathrm{I}, z_\mathrm{II}) = (\Phi_P(x_\mathrm{I}, x_\mathrm{II}) - M_m^2) \chi^d_c(x_\mathrm{I}, x_\mathrm{II}) \xi^p_r(z_\mathrm{I}, z_\mathrm{II}) \tag{A8}$$

Multiplication of (A1a) by (A2b) and (A1b) by (A2a) leads to products of the form $\chi_{Ab}(x_\mathrm{I}) \psi_{B\dot{e}}(x_\mathrm{II})$ and $\psi^a_A(x_\mathrm{I}) \chi^f_B(x_\mathrm{II})$, which after generalizations of the type (A5a) transform like diquarks. Since such objects, like quarks, are not observable, they are consistently put to zero. Observing this in the product of (A3a) and (A3b) leads to

$$\Box_\mathrm{I} \Box_\mathrm{II} \Phi_P(x_\mathrm{I}, x_\mathrm{II}) = \tfrac{1}{2} \mathrm{Re}(\psi^a_b(x_\mathrm{II}, x_\mathrm{I}) \chi^b_a(x_\mathrm{II}, x_\mathrm{I})) \tag{A9}$$

where $\chi^b_a = (\chi^b_a)^*$. Multiplication of (A3) by (A1) or (A2) also leads to zero contribution by the same reasoning as above.

Equations (A7)–(A9) are the meson equations (I 5.4), (I 5.5), and (I 4.12), which are manifestly Lorentz invariant by virtue of their spinor form. Justification of these equations does not come from the above construction, but has to come from confrontation with data. To date, such confrontations have been somewhat limited in scope but successful in many different areas of basic importance mentioned in the references. No major and basic contradiction to data has so far been encountered.

The meson equations (A7)–(A9) have been converted into the action integral (III A4) and (3.1) of ref. 8.

ACKNOWLEDGEMENT

My association with the High Energy Division of the Department of Radiation Sciences, Uppsala University during the past year is duefully acknowledged.

REFERENCES

1. Particle Data Group, (1996), *Phys. Rev. D* **54**(1).
2. Weinberg, S. (1979). *Physica A* **96**, 327.
3. Gasser, J., and Leutwyler, H. (1985). *Nucl. Phys. B* **250**, 465, 517.
4. Harada, M., and Schechter, J. (1996). *Phys. Rev. D* **54**, 3394.
5. Cheng, H-Y., *et al.* (1994). *Phys. Rev. D* **49**, 2490.
6. Casalbuoni, R., *et al.* (1992). *Phys. Lett. B* **294**, 106.
7. Hoh, F. C. (1993). *Int. J. Theor. Phys.* **32**, 1111 [denoted by I].
8. Hoh, F. C. (1994). *Int. J. Mod. Phys.* **A9**, 365.
9. Hoh, F. C. (1996). *J. Phys. G.* **22**, 85.
10. Hoh, F. C. (1997). *Int. J. Theor. Phys.* **36**, 509 [denoted by II].
11. Hoh, F. C. (1998). *Int. J. Theor. Phys.* **37**, 1693.
12 Hoh, F. C. (1999). Radiative decay of vector meson $V \rightarrow P\gamma$ in the spinor strong interaction theory, *Int. J. Theor. Phys.*, this issue [denoted by III].
13. Dally, E. B., *et al.* (1977). *Phys. Rev. Lett.* **39**, 1176; (1980). *Phys. Rev. Lett.* **45**, 232; (1982). *Phys. Rev. Lett.* **48**, 375.
14. Bebek, C. J., *et al.* (1978). *Phys. Rev. D* **17**, 1693.
15. Hoh, F. C. (1994). *Int. J. Theor. Phys.* **33**, 2325.
16. Frank, M. and O'Donnell, P. J. (1985). *Phys. Lett. B* **159**, 174.
17. Wick, G. C. (1954). *Phys. Rev.* **96**, 1124.